# Benzene polycarboxylic acid characterisation of polyaromatics in ambient aerosol: Method development

Some of the authors of this publication are also working on these related projects:

Monitoring and Sources Assessment of Persistent Organic Pollutants in Nepal:Implication on human health View project

Towards an Air Toxic Management SYstem in China (ATMSYC) View project

# Molecular marker study of aerosols in the northern South China Sea: Impact of atmospheric outflow from the Indo-China Peninsula and South China

Xiaofei Geng[a,b], Guangcai Zhong[a,*], Jun Li[a], Zhineng Cheng[a], Yangzhi Mo[a], Shuduan Mao[a], Tao Su[a], Haoyu Jiang[a], Kaiwen Ni[c], Gan Zhang[a]

[a] State Key Laboratory of Organic Geochemistry, Guangzhou Institute of Geochemistry, Chinese Academy of Sciences, Guangzhou, 510640, China
[b] University of Chinese Academy of Sciences, Beijing, 100049, China
[c] South China Agricultural University, Guangzhou, 510642, China

## ABSTRACT

Continental outflow influences concentration and chemical composition of marine aerosols, which has an important impact on regional biogeochemistry and climate. Aerosols sampling for molecular marker study was conducted from June 2015 to May 2016 at Xieyang Island in the northern South China Sea (SCS), to learn the impact of outflow from Indo-China Peninsular (ICP) and South China (SC). Xieyang Island was under the influence of air masses from ICP and SC nearly 70% of the year. Levels of anhydrosugars were higher during October to early March. They were lower in April and May, although biomass burning events in ICP were most intensive and half of air masses back trajectories passed through ICP in this period. Significant correlations between levels of anhydrosugars, polycyclic aromatic hydrocarbons, *n*-alkanes, high molecular weight *n*-fatty acids and terephthalic acid were observed, suggesting co-emissions of these compounds. Source types of aerosol primary organic matter (POM) tracked by these markers, namely open burning of municipal wastes, fossil fuel combustion, higher plant emissions and biomass burning, largely contributed in fall and winter with SC to be an important source region. However, levels of sugar alcohols (a group of biogenic aerosol tracers) were higher in warm seasons with ICP and SCS to be the main source regions, and were poorly correlated with levels of other molecular markers. Carbon preference index of *n*-alkanes also increased in warm seasons, indicating enhanced higher plant wax emissions. It suggested that there was a close link between biogenic emissions of sugar alcohols (or *n*-alkanes) and the growing activities of related organisms. Besides continental outflow, there were marine sources of steranes, hopanes (fossil sources tracers) and mannitol (a sugar alcohol), since their levels were higher for aerosol samples basically influenced by air masses originated from SCS.

## 1. Introduction

Covering about 70.9% of the Earth's surface, oceans are important source regions of natural aerosols (O'Dowd and de Leeuw, 2007). Marine aerosols can significantly alter the global cloud condensation nuclei budget and hence affect water cycle and climate of the world (O'Dowd and de Leeuw, 2007; Penner et al., 2001). Carbonaceous aerosols account for a significant fraction of marine aerosols (O'Dowd and de Leeuw, 2007; O'Dowd et al., 2004). In addition to emissions originated from the oceans, continental outflow is also an important source of carbonaceous aerosols in marine environment (Feng et al., 2007; Fu et al., 2011; O'Dowd and de Leeuw, 2007; Zhao et al., 2016).

Asia continent is one of the most important source region of atmospheric aerosols (Ramanathan and Crutzen, 2003). Fossil fuel combustion and biomass burning are two major anthropogenic sources of carbonaceous aerosols in Asia continent (Feng et al., 2007; Zhao et al., 2016). The Indo-China Peninsula (ICP), including Myanmar, Thailand, Vietnam, Laos and Cambodia, is one of the regions with most intensive biomass burning activities in the world (Lin et al., 2013). Agricultural burning starts from late winter and peaks in spring every year (Lin et al., 2009). Such burnings mostly are forest fires and crop residue burning taking place at open field and can be clearly showed by satellite images of fire counts (Fig. S1) (Lin et al., 2009; Shi and Yamaguchi, 2014). China has a great consumption of coal for industry and petroleum for vehicles, but biomass burning is also popular in this region by means of crop residue burning and domestic biofuel burning (Streets et al., 2003; Lai et al., 2016).

The South China Sea (SCS) is a marginal sea surrounded by ICP and

---

South China (SC). There have been few studies on continental outflow of aerosols from ICP and SC to SCS, especially for carbonaceous aerosols (Atwood et al., 2013; Chuang et al., 2013; Pani et al., 2016; Xiao et al., 2017; Zhao et al., 2016; Zheng et al., 2018). Some studies on continental outflow of carbonaceous aerosols to SCS only covered a short period (no longer than one season) (Zhao et al., 2016; Song et al., 2018; Zheng et al., 2018). Composition and sources of carbonaceous aerosols in SCS are still not well understood.

The analysis of organic molecular markers is a typical way to trace sources of aerosols. Anhydrosugars (levoglucosan, galactosan and mannosan) are derived from pyrolysis of cellulose and are widely used as typical tracers of biomass burning (Fraser and Lakshmanan, 2000; Mochida et al., 2010; Nolte et al., 2001). Lipid compounds, hopanes, steranes and polycyclic aromatic hydrocarbons (PAHs) are also useful tracers for sources including fossil fuel combustion, higher plant waxes emissions, microorganism and marine plankton emissions (Fu et al., 2011; Simoneit, 1989). Levels of molecular markers were commonly used as inputs to receptor models (such as positive matrix factorization, PMF) for source apportionment of aerosols (Jaeckels et al., 2007).

To improve our understanding of continental outflow of carbonaceous aerosol from ICP and SC to SCS, year-round aerosol sampling for molecular marker study was conducted from June 2015 to May 2016 on a small coastal island (i.e. Xieyang Island, Fig. 1) in the northern SCS. There are few human activities on the island, what makes it an ideal site to study aerosols outflow from ICP and SC. Contributions of different source types to primary organic matter (POM) in carbonaceous aerosols were estimated based on molecular markers and PMF analysis. These results combining with air masses back trajectory and potential source contribution function (PSCF) model analysis were used to investigate typical source regions of each source type.

## 2. Experimental section

### 2.1. Sample collection

The Xieyang Island (Fig. 1) is a coastal island of $1.89 \, \text{km}^2$ in northern SCS. There are only dozens of people living on the island as fishermen. Local pollution is expected to be very little. Most regions of the island are hilly with highest elevation of 149 m above sea level (ASL). Our sampling site ($20.908°N$, $109.214°E$) was located at a concrete platform of a hill of Xieyang Island. Elevation of our sampling site was 80 m ASL. Residence of people on the island concentrates in a small region at lower elevations.

Atmospheric fine particle ($PM_{2.5}$) samples were collected on microquartz fiber filters (Munktell, $203 \times 254 \, \text{mm}$, pre-combusted at 500 °C for 6 h) by a high volume air sampler in flow rate of $1 \, \text{m}^3 \, \text{min}^{-1}$ for about 24 h. One sample was taken every week from June 2015 to February 2016 to obtain 40 samples. Two samples were taken every week from March to May 2016 to obtain 29 samples. Filter samples were wrapped in prebaked aluminum foils, packed in airtight polyethylene bags and stored at $-20 °C$ prior to analysis.

### 2.2. Thermal-optical carbon analysis

Each filter sample was punched in size of $0.544 \, \text{cm}^2$ for analysis of organic and elemental carbon (OC and EC) by using a thermal-optical carbon analyzer (Atmoslytic Inc., Calabasas, CA) following the IMPROVE_A thermal-optical reflectance (TOR) protocol. More details can be found in the reference (Zong et al., 2016). The detection limits of this method were 0.82 and $0.20 \, \mu\text{g} \, \text{cm}^{-2}$ for OC and EC, respectively. Relative standard deviations of replicate analysis were ~1.0% for OC, EC and TC. OC and EC were undetectable in field filter blanks.

### 2.3. Non-polar organics analysis

Non-polar organic molecular markers such as PAHs (fluoranthene (Flua), pyrene (Pyr), benzo[a]anthracene (BaA), chrysene (Chr), benzo[b]fluoranthene (BbF), benzo[k]fluoranthene (BkF), benzo[a]pyrene (BaP), dibenzo[a,h]anthracene (DahA), benzo[g,h,i]perylene (BghiP) and indeno[1,2,3-c,d]pyrene (Ind)), $n$-alkanes ($C_{23}$–$C_{35}$), steranes and hopanes ($\alpha\alpha\alpha$ 20R 24R-ethylcholestane, 17$\alpha$(H),21$\beta$(H)-22-homohopane, 17$\alpha$(H),21$\beta$(H)–22S-homohopane and $\alpha\beta\beta$ 20R 24R-ethylcholestane) were quantified by gas chromatograph mass spectrometer (SHIMADZU, GCMS-QP2010) equipped with a DB-5MS column
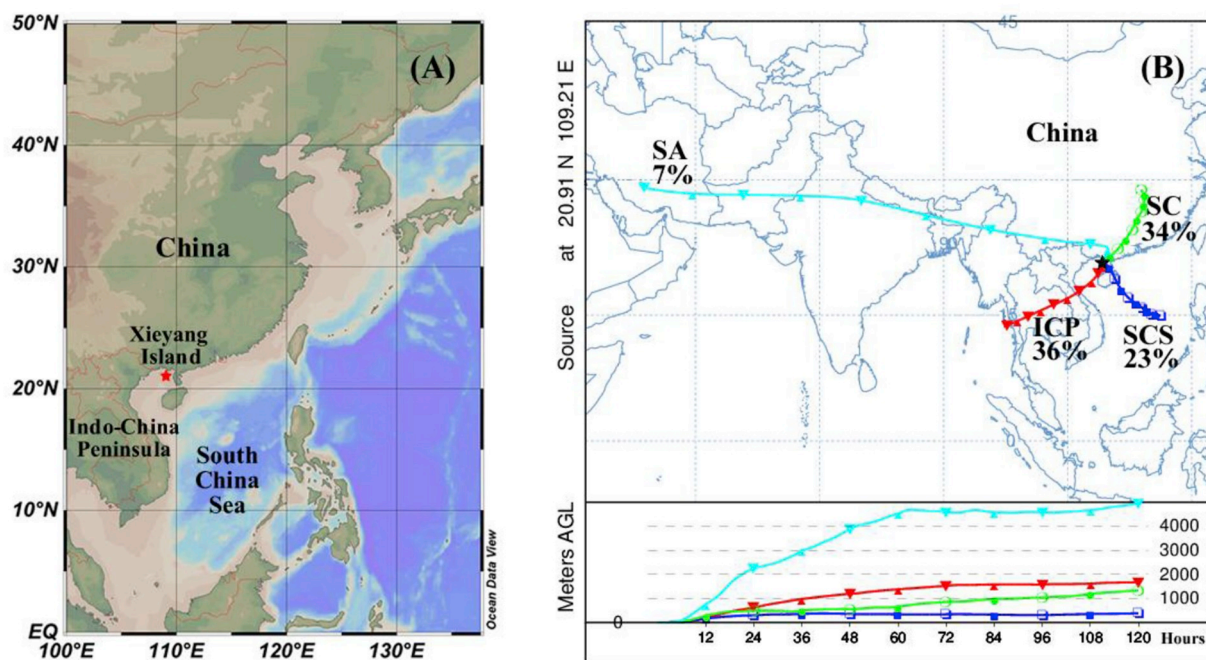


**Fig. 1.** Geographical location of Xieyang Island (marked with a red star) in the northern South China Sea (A) and clusters of air mass back trajectories from June 2015 to May 2016 (B). SA: South Asia; AGL: above ground level. (For interpretation of the references to colour in this figure legend, the reader is referred to the Web version of this article.)

(Agilent, 30 m × 0.25 mm × 0.25 μm). Surrogates of PAHs (phenanthrene-$d_{10}$, chrysene-$d_{12}$, perylene-$d_{12}$), *n*-alkanes, steranes and hopanes (*n*-tetracosane-$d_{50}$) were added to check the recoveries before 24-h Soxhlet extraction of the filter samples with dichloromethane (DCM). The extract was concentrated to about 1 mL by a rotary evaporator afterwards. The concentrated extract was then loaded onto a glass column packed with anhydrous sodium sulfate, neutral silica gel and neutral alumina, and eluted with 20 mL DCM/hexane (1:1, v:v). The eluate was further concentrated to 50 μL under gentle stream of high purity nitrogen. Prior to GC-MS analysis, hexamethylbenzene was added as internal standard.

PAHs concentrations were corrected by recoveries of PAHs surrogates (60%–110%). Concentrations of *n*-alkanes, steranes and hopanes were not corrected by recoveries of their surrogate (100 ± 6%). Along with the analysis of field samples, seven laboratory blanks were analysed too. The method detection limits (MDLs) were defined as average of laboratory blanks plus three times standard deviations of laboratory blanks. The detected non-polar organics in field blanks were below MDLs, so the results were not corrected by field blanks.

### 2.4. Polar organics analysis

Polar organics were analyzed, including biomass burning tracers (galactosan, mannosan, levoglucosan, vanillin, syringic acid, vanillic acid), sugar alcohols (mannitol, arabitol and erythritol), *n*-fatty acids ($C_{10}-C_{30}$), oleic acid and terephthalic acid. Briefly, filter samples were spiked with internal standards (methyl-β-D-xylopyranoside and palmitic acid-$d_{31}$) before 36-h Soxhlet extraction using DCM/methanol (93:7, v:v). Anhydrous sodium sulfate was added into the extracts to remove water.

The extracts were concentrated using a rotary evaporator, dried under gentle stream of high purity nitrogen. Derivatization of the polar organics was done by adding 200 μL N,O-bis-trimethylsilyl-trifluoroacetamide (1% trimethylchlorosilane) and 100 μL anhydrous pyridine, followed by heating at 70 °C for 1 h. After derivatization, the samples were dried under nitrogen blowing. Hexane (200 μL) was added prior to measurment using GC-MS (Agilent GC7890 A coupled with 5975C MSD) equipped with a DB-5MS column (30 m × 0.25 mm × 0.25 μm). The recoveries of polar organics ranged from 69% to 113%. Concentrations of polar compounds were not recovery-corrected but corrected by field blanks.

### 2.5. Air masses back trajectories

Five-day backward trajectories were generated by Hybrid Single-particle Lagrangian Integrated Trajectory (HYSPLIT) model (http://www.arl.noaa.gov/HYSPLIT.php). The applied meteorological data were obtained from Gridded Meteorological Data Archives of Air Resources Laboratory (ARL) (http://ready.arl.noaa.gov/archives.php). All trajectories ending at the sampling site (2 m above ground level) were calculated at 2 h intervals during the 24 h sampling period. Clustering trajectories of all samples showed that Xieyang Island was under the influence of air masses from ICP and SC nearly 70% of the year (Fig. 1).

### 2.6. Positive matrix factorization (PMF)

Details of PMF analysis were described in the Supplement. PMF has been widely used in source apportionment of aerosols (Jaeckels et al., 2007). Concentrations of species and corresponding uncertainties are required for performing PMF model. Furthermore, considering that the uncertainty plays a key role in application of PMF model, an appropriate level of uncertainty should be taken seriously. For the species above MDLs, the uncertainties were calculated by square root of the sum of squares of detection limits, and the products of detected concentrations and corresponding relative uncertainies of the compounds

estimated from the analytical error (Choi et al., 2015; Qadir et al., 2013). The values below MDLs were replaced by the half of detection limits with uncertainties of 5/6 detection limits (Choi et al., 2015; Hovorka et al., 2015). Missing data were approximated as the geometric means of corresponding compounds and the uncertainties were assigned to four times the geometric means (Choi et al., 2015; Polissar et al., 1998; Shrivastava et al., 2007).

In order to get the source profiles of POM, EPA PMF 5.0 model was applied. POM level was set as a total variable and was obtained from organic carbon content by multiplying a factor of 1.8 (Turpin and Lim, 2001). The chemical species applied to PMF analysis including *n*-alkanes ($C_{23}-C_{35}$), steranes and hopanes, PAHs, *n*-fatty acids ($C_{10}$-$C_{30}$), terephthalic acid, anhydrosugars, vanillin, vanillic acid, syringic acid, oleic acid and sugar alcohols. For some species, the percentage of values below detection limits peaked at 28%, and the missing data accounted for up to 4%.

To physically find out the reasonable results and a model method matched well with the data, 3 to 7 factors were tested. Considering Q values, scaled residuals and source profiles, 5 factors were chosen to interpret the source profiles. The key basis of choosing optimum factors was interpretability, which was defined by how PMF apportioned source-class-specific groups of molecular markers (Shrivastava et al., 2007). A four-factor model was rejected as it set tracers of higher plant wax and waste incineration into one group. A six-factor model was also rejected because erythritol was taken out of the group of microbial activities to form a separate factor without other chemical species' support. A five-factor model was adopted as it had distinctive groupings of chemical species and logical explanation of 85.7% of POM.

### 2.7. Potential source contribution function (PSCF)

Based on the HYSPLIT model, PSCF was widely applied to source identification and appointment (Jain et al., 2017; Li et al., 2017; Zhang et al., 2010) by dividing the potential source area into grid cells of $i \times j$. The *ij*th component of a PSCF field is defined as:

$$\text{PSCF}_{ij} = \frac{m_{ij}}{n_{ij}}$$

Where $\text{PSCF}_{ij}$ is the possibility of air parcel loaded with species of high concentrations originating from the *ij*th cell. $n_{ij}$ represents the number of trajectory endpoints fall in the *ij*th cell and $m_{ij}$ is the number of air masses, from the same cell, loaded with species whose concentrations are greater than the corresponding criterion values. Generally, $\text{PSCF}_{ij}$ ranged from 0 to 1. And the higher the $\text{PSCF}_{ij}$ value is, the greater possible the source region is. In this study, PSCF model was performed to identify potential source regions of source profiles derived from PMF analysis, and the threshold values were set as the 75th percentile of corresponding factors.

## 3. Results and discussion

### 3.1. Anhydrosugars

Levoglucosan, galactosan and mannosan are products of cellulose pyrolysis (Simoneit et al., 1999). They have been used as molecular markers of biomass burning aerosols in many studies (Fu et al., 2011; Jiang et al., 2018; Simoneit et al., 1999). In the present study, mean concentration of levoglucosan (20.54 ± 35.86 ng m$^{-3}$) was higher than those of galactosan (0.95 ± 1.62 ng m$^{-3}$) and mannosan (1.59 ± 2.71 ng m$^{-3}$). Mean levoglucosan level in our study was significantly higher than those observed in remote marine aerosols from the Arctic and western North Pacific (Table 1) (Chen et al., 2013; Fu et al., 2013; Kawamura et al., 2003). However, it was much lower than those previously reported for aerosols from regions supposed to be closer to biomass burning emission sources in ICP or SC, namely Sonla in northern Vietnam and Guangzhou in SC (Table 1) (Nguyen et al.,

**Table 1**
Comparison of molecular markers' mean concentrations (unit: ng m$^{-3}$) of our study with those reported for other regions.

| Sampling region | Period | Levo | n-alkanes | HFAs | LFAs | References |
|---|---|---|---|---|---|---|
| Arctic Ocean* | 2009.08 | 0.37 ± 0.36 | 0.82 ± 1.3 ($C_{18}$–$C_{34}$) | 0.58 ± 0.06 ($C_{20}$–$C_{32}$) | 2.34 ± 0.33 ($C_8$–$C_{19}$) | Fu et al. (2013) |
| Western North Pacific* | 1990.04–1993.11 | 0.62 | 1.8 ($C_{20}$–$C_{36}$) | 3.5 ± 2.3 ($C_{20}$–$C_{32}$) | 10.4 ± 8.2 ($C_{12}$–$C_{19}$) | (Chen et al., 2013; Kawamura et al., 2003) |
| | 2006.01–2010.01 | 0.54 | – | – | – | |
| East China Sea* | 2014.05–06 | – | 47.1 ± 37.0 ($C_{19}$–$C_{36}$) | 14.3.4 ± 18.9 ($C_{20}$–$C_{32}$) | 72.6 ± 47.0 ($C_8$–$C_{19}$) | Kang et al. (2017) |
| Hong Kong, South China** | winter 2003 | 130 | 195 ($C_{16}$–$C_{35}$) | 54.8 ($C_{20}$–$C_{34}$) | 169.6 ($C_9$–$C_{19}$) | (Wang et al., 2006; Zhao et al., 2014) |
| | summer 2003 | 6.2 | 10 ($C_{16}$–$C_{35}$) | 5.7 ($C_{20}$–$C_{34}$) | 170 ($C_9$–$C_{19}$) | |
| Guangzhou, South China** | winter 2003 | 848 | 994 ($C_{16}$–$C_{35}$) | 301.7 ($C_{20}$–$C_{34}$) | 961.6 ($C_9$–$C_{19}$) | |
| | summer 2003 | 49 | 155 ($C_{16}$–$C_{35}$) | 26.9 ($C_{20}$–$C_{34}$) | 427.5 ($C_9$–$C_{19}$) | |
| | 2009.11–12 | 118 | – | 32.04 ($C_{20}$–$C_{32}$) | 154 ($C_{14}$–$C_{19}$) | |
| Sonla, Northern Vietnam** | 2013.02–04 | 1620 ± 893 | – | – | – | Nguyen et al. (2016) |
| Xieyang Island** | 2015.06–2016.05 | 20.54 ± 35.86 | 37.82 ± 40.25 ($C_{23}$–$C_{35}$) | 81.69 ± 101.47 ($C_{20}$–$C_{30}$) | 39.07 ± 37.00 ($C_{10}$–$C_{18}$) | our study |

*data for total suspended particles;
**data for PM$_{2.5}$; Levo: levoglucosan; HFAs: high molecular weight fatty acids; LFAs: low molecular weight fatty acids;
–: mean concentration of the sampling period was not given.

2016; Zhao et al., 2014). It was also slightly lower than mean levoglucosan level of aerosols from a background site on Hainan Island of China (42 ± 33 ng m$^{-3}$) (Zhang et al., 2012), which is also an island in SCS as Xieyang Island but with much larger area (35,400 km$^2$) and population (9.25 millions).

Temporal variation of anhydrosugars could be resulted from difference of source regions and difference of biomass burning intensity of the source regions in different periods. During June to September, open biomass burning events were most intensive in China but much less popular in ICP based on MODIS fire count data (Fig. S1). Air masses arriving at our sampling site originated mostly from ICP and just occasionally from China in this period (Fig. 2A). Thus, relatively low levels of anhydrosugars were observed during June to September (Fig. 3).

Open biomass burning events in ICP started to increase since December, then reached its maximum in March and April, and started to decrease since May (Fig. S1). It was interesting that low levels of anhydrosugars were observed during April and May (Fig. 3), even though open biomass burning events were very popular in ICP and 46% of air masses back trajectories passed through ICP in this period (Fig. 2D). Previous studies have proposed a transport mechanism of biomass burning pollutants from ICP to East Asia involving uplift of the pollutants and further transport by westerly winds at high altitudes (Lin et al., 2009, 2013). The pollutants at high altitudes could be monitored at locations with high elevations, as reported for the Mountain Lulin site in Taiwan (2862 m ASL) (Lee et al., 2011). The pollutants also could reach low elevations under strong downward wind conditions and be detected, as reported for southern Taiwan and Hong Kong (Chan, 2017; Yen et al., 2013). However, this case was not observed for the continuous aerosols measurement at Dongsha Island in the SCS (Atwood et al., 2013). Low anhydrosugars' levels observed during April and May in our study was likely due to uplift of biomass burning aerosols from ICP, as well as a lack of strong downward wind to bring down the aerosols at high altitudes to our sampling site at low elevation.

Elevated concentrations of anhydrosugars were observed at Xieyang Island during October to early March (Fig. 3). In this period, SC was the main source region of anhydrosugars, because air masses back trajectories largely passed through SC (Fig. 2B and C). The MODIS fire count data showed that open biomass burning events in China were moderate in October, February and March, but very little from November to January (Fig. S1). MODIS fire count data was not able to reflect indoor biomass burning activities. High concentrations of anhydrosugars were

still found from November to January, suggesting that indoor biofuel combustion for domestic heating was popular in cold season. Anhydrosugars' levels peaked in February, which seems attributed to both open biomass burning and domestic biofuel combustion. Firstly, comparing with October, open biomass burning events in February were more concentrated in SC (Fig. S1), which was closer to our sampling site. Secondly, open biomass burning was more popular in February than in November to January. Thirdly, domestic biofuel combustion was probably still intensive in China until February, but less popular in March due to the warmer weather.

Generally, the ratio of levoglucosan and mannosan (L/M) as well as the ratio of mannosan and galactosan (M/G) can be used to distinguish biomass burning aerosols from different types of biomass, since L/M and M/G ratios do not change significantly with burning temperature (Fabbri et al., 2009). In the present study, L/M and M/G ratios of aerosols from burning of different types of biomass were compiled based on results from previous studies on emission inventories (Bari et al., 2009; Engling et al., 2006, 2009; Fine et al., 2001, 2002; Oros et al., 2006; Schmidl et al., 2008; Sullivan et al., 2008). L/M and M/G ratios were calculated for individual aerosol samples, whose corresponding air mass back trajectories mainly originated from SC or ICP (Fig. 4). The results showed that burning of all types of biomass (namely softwoods, hardwoods and herbaceous plant) was common in ICP, whereas burning of softwoods was not frequent in SC (Fig. 4).

### 3.2. Steranes and hopanes

Steranes and hopanes exist in coal and crude oil (Oros and Simoneit, 2000; Rogge et al., 1993). It was found that motor vehicles dominated contributions of steranes and hopanes in atmosphere in urban areas, so these compounds have been used as molecular markers of vehicle emissions (Hildemann et al., 1991; Schauer et al., 1999). Steranes and hopanes are present in fuel and lubricating oil, and released by both gasoline-powered and diesel-powered motor vehicles (Kleeman et al., 2008; Schauer et al., 1999). Concentration ratios of hopanes to steranes ($R_{h/s}$) can be used to show difference of source types (Feng et al., 2007). In the present study, $R_{h/s}$ fell within a narrow range from 0.13 to 0.27 (0.20 ± 0.03) in the whole sampling year, which suggested that there was little temporal variation of source types of steranes and hopanes.

Levels of steranes and hopanes were found to be obviously higher for samples mainly influenced by air masses from SCS (Fig. 5). This
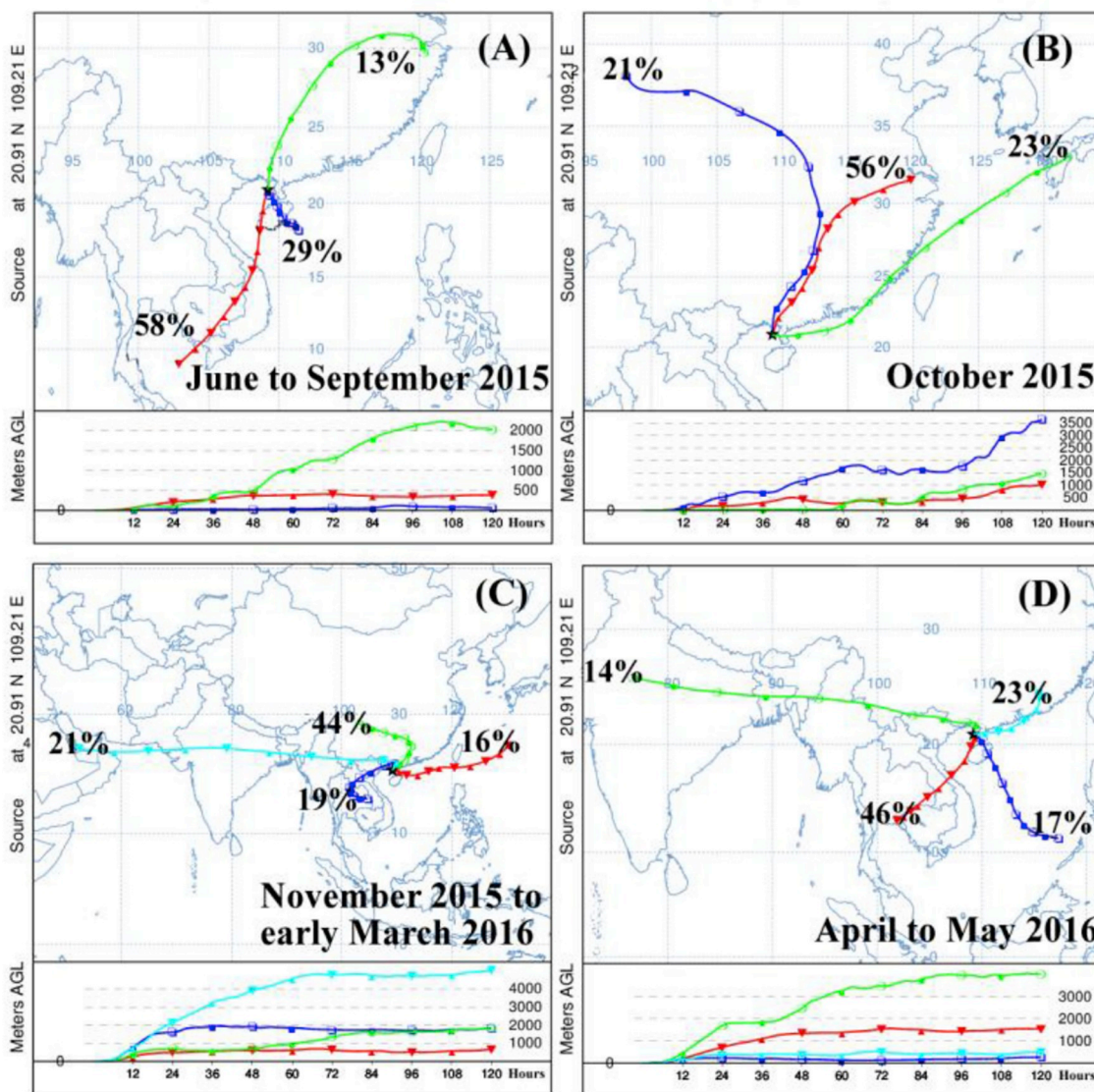
Fig. 2. Back trajectories in June to September 2015 (A), October 2015 (B), November 2015 to early March 2016 (C) and April to May 2016 (D).

showed a marine source of steranes and hopanes. Shipping emissions have been recognized to be an important source of atmospheric fine particle pollution in recent years (Zhang et al., 2017). The SCS is host to some of the world's busiest international sea lanes. The Pearl River Delta in SC is home to three of ten busiest ports in the world. Besides international sailing vessels, fishing boats are also a main contributor of shipping emissions in China, especially in its southern coastal areas (Zhang et al., 2017, 2018). Ships are typically equipped with diesel-powered engines, which are known for their high emissions of carbonaceous aerosols (Eichler et al., 2017). Lubricating oil used for the ships is also a major constituent of ship exhaust particles (Eichler et al., 2017). In our study, shipping emissions were likely the main source of steranes and hopanes for samples mainly influenced by air masses from SCS, so $R_{h/s}$ of these samples represented a petroleum signature (e.g. diesel and lubricating oil) but not coal. Since narrow range of $R_{h/s}$ has been observed for all samples, continental outflow of steranes and hopanes from ICP and SC was likely attributed to petroleum sources too.

### 3.3. PAHs

PAHs in ambient aerosols are derived from petrogenic sources or incomplete combustion of biomass and fossil fuels (Tobiszewski and

Namiesnik, 2012). Concentrations of PAHs in our study ranged from 0.12 to 12.26 ng m$^{-3}$. The mean concentration (1.74 ± 1.91 ng m$^{-3}$) was similar as levels of PAHs in aerosols collected from SCS during a cruise in 2007 (∼1–3 ng m$^{-3}$) (Liu et al., 2014). Diagnostic ratios of PAHs were used in previous studies to differentiate source types releasing PAHs (Table 2) (Leung et al., 2014; Tobiszewski and Namiesnik, 2012). The ratios of BaA/(BaA + Chr), IcdP/(IcdP + BghiPe) and Flua/(Flua + Pyr) showed that petrogenic sources contributed insignificantly to PAHs in our study (Table 2). The BaA/(BaA + Chr) values indicated coal combustion sources. However, the IcdP/(IcdP + BghiPe) and Flua/(Flua + Pyr) values were close to the cutoff values of petroleum combustion sources and grass, wood and coal combustion sources. So significance of these sources' contributions cannot be further estimated by diagnostic ratios.

There was a very significant correlation between levels of PAHs and anhydrosugars ($r = ∼0.8$, $p < 0.01$, Table 3), but it could not reach a conclusion that biomass burning was an important source of PAHs. Anhydrosugars' levels also significantly correlated with those of terephthalic acid, which is a molecular marker of plastics combustion ($r = ∼0.8$, $p < 0.01$). Actually, levels of many molecular markers were significantly correlated with each other, including n-alkanes, high molecular weight n-fatty acids, PAHs, terephthalic acid and
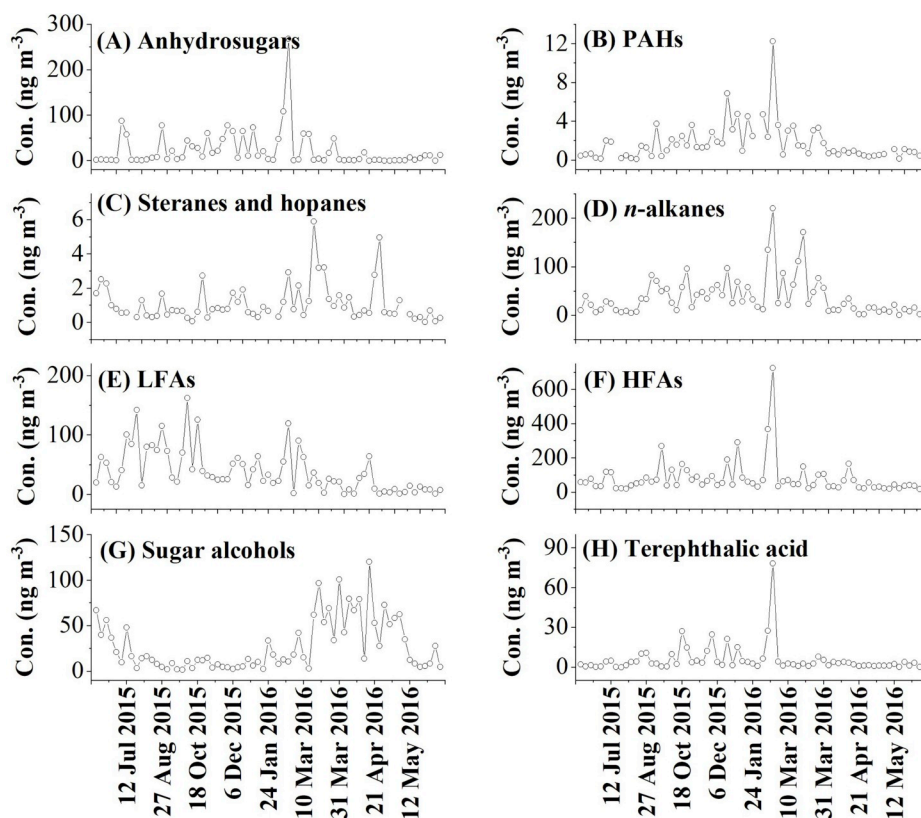
**Fig. 3.** Temporal variations of molecular markers' concentrations (y-axis). HFAs: high molecular weight *n*-fatty acids; LFAs: low molecular weight *n*-fatty acids.

anhydrosugars ($r \geq 0.6$, $p < 0.01$, Table 3). These good correlations indicated co-emissions of these chemicals from similar source regions, but they might be from different source types. Weak correlation was observed for PAHs' levels and levels of steranes and hopanes (Table 3). PAHs' levels were higher for aerosol samples mainly influenced by air masses from SC and ICP (Fig. 5). This case was different from that of steranes and hopanes, as mentioned in Section 3.2. Thus, PAHs of our sampling site were contributed more by continental outflow compared to shipping emissions.

### 3.4. n-Alkanes

*n*-Alkanes ($C_{23}$–$C_{35}$) in aerosols are emitted from terrestrial higher plant waxes and incomplete combustion of fossil fuels. Average level of *n*-alkanes in our study was lower than those reported for two coastal cities (i.e. Guangzhou and Hong Kong) in SC (Table 1) (Wang et al., 2006; Zhao et al., 2014), but was higher than that found in the western North Pacific and comparable to that of East China Sea (Table 1) (Chen et al., 2013; Kang et al., 2017). Carbon preference index (CPI) is the ratio between concentrations of odd and even carbon number *n*-alkanes. CPI can be used to distinguish source types of *n*-alkanes. CPI values are about 5–10 for *n*-alkanes from terrestrial higher plant waxes, but are close to unity for *n*-alkanes from incomplete combustion of fossil fuels (Fu et al., 2011; Kawamura et al., 2003). Mean CPI value was $1.83 \pm 0.63$ in our study, excluding an outlier (9.08). The molecular distributions of *n*-alkanes peaked at $C_{27}$. Generally, lower molecular weight *n*-alkanes ($C_{20}$-$C_{26}$) are derived from incomplete combustion of fossil fuels, while higher molecular weight *n*-alkanes ($\geq C_{27}$) are derived from higher plant waxes (Fu et al., 2011; Kawamura et al., 2003). It suggested that *n*-alkanes in aerosols of Xieyang Island were from both terrestrial higher plant waxes and incomplete combustion of fossil fuel, but the latter was dominant.

As we mentioned in Section 3.3, PAHs were more likely from continental outflow, while steranes and hopanes were partly contributed

by shipping emissions. There was a good correlation between levels of *n*-alkanes and PAHs ($r = 0.62$, $p < 0.01$). Significant correlation was also observed for levels of *n*-alkanes and steranes and hopanes ($r = 0.44$, $p < 0.01$). It seems emissions from both continental outflow and shipping deserved attention for *n*-alkanes. As shown in Fig. 5, mean concentration of *n*-alkanes for samples influenced by air masses from SCS were lower than that for samples influenced by air masses from SC, but was still higher than that for samples influenced by air masses from ICP.

There was a clear increasing trend of CPI values (namely contribution of higher plant waxes emissions to *n*-alkanes) from November to May, and a clear decreasing trend from June to September (Fig. 6). There was little difference among CPI values of aerosol samples influenced by air masses from ICP ($2.02 \pm 0.70$), SCS ($1.97 \pm 0.83$) and SC ($1.64 \pm 0.39$). It meant that contributions of terrestrial higher plant waxes emissions were independent of source regions. The emissions probably were closely linked with climate parameters like temperature, which affected plant growing activities.

### 3.5. n-Fatty acids

High and low molecular weight *n*-fatty acids (HFAs and LFAs) in ambient aerosols are released from different source types. HFAs are from terrestrial higher plant waxes (Medeiros et al., 2006; Simoneit, 1977). LFAs are derived from anthropogenic activities (e.g., fossil fuel combustion, biomass burning and cooking) and biogenic (e.g., microorganism and marine plankton) emissions (Fine et al., 2001; Kawamura et al., 2003; Rogge et al., 1993; Rogge et al., 1991; Zhao et al., 2007a, b). Mean concentration of HFAs ($C_{20}$-$C_{30}$) in our study ($81.69 \pm 101.47\ \mathrm{ng\,m^{-3}}$) was higher than those for aerosols in the Arctic and Pacific Oceans, as well as the East China Sea (Table 1). As mentioned in Section 3.4, the contribution of terrestrial higher plant waxes emissions to *n*-alkanes enhanced in warm periods. However, HFAs' levels did not increase in warm periods. It might be because
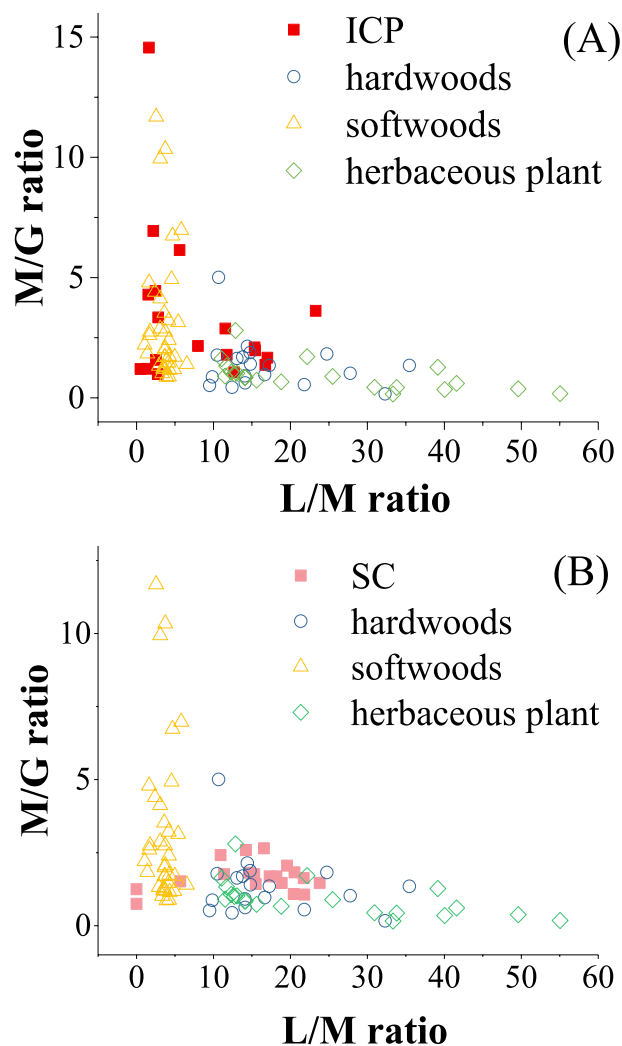
**Fig. 4.** Scatter plots of levoglucosan/mannosan concentration ratios (L/M) (x-axis) versus mannosan/galactosan concentration ratios (M/G) (y-axis) for biomass burning sources (hollow dots) and aerosol samples basically influenced by air mass originated from ICP and SC (solid dots).

biomass burning also contributed to HFAs.

Mean concentration of LFAs ($C_{10}$-$C_{18}$) in our study ($39.07 \pm 37.00 \, \mathrm{ng \, m^{-3}}$) was also higher than those for the Arctic and Pacific Oceans (Chen et al., 2013; Fu et al., 2013), but lower than that for the East China Sea (Kang et al., 2017). The latter is adjacent to eastern China, where population was huge and anthropogenic emissions were intensive. Although there could be marine sources of LFAs, LFAs' levels were lower for samples mainly influenced by air masses from SCS (Fig. 5).

### 3.6. Sugar alcohols

The sugar alcohols (mannitol, arabitol and erythritol) are mainly released by biogenic sources like fungi, bacteria, marine plankton and lower plants (Bauer et al., 2008; Burshtein et al., 2011; Gosselin et al., 2016). In the present study, mannitol and arabitol ($12.26 \pm 15.05$ and $8.67 \pm 10.70 \, \mathrm{ng \, m^{-3}}$, respectively) were more abundant than erythritol ($6.68 \pm 7.26 \, \mathrm{ng \, m^{-3}}$), similar as results of two remote islands (Okinawa and Chichijima Islands) in western North Pacific (Chen et al., 2013; Verma et al., 2018; Zhu et al., 2015). Sugar alcohols showed weak correlation with other molecular markers obviously contributed by continental outflow (i.e. PAHs, terephthalic acid and anhydrosugars, Table 3). They show distinctive temporal variations with high levels in

spring and summer (March to July) and low levels in fall and winter (August to December, Fig. 3). There were high levels of sugar alcohols in summer in Okinawa and Chichijima Islands too (Chen et al., 2013; Verma et al., 2018; Zhu et al., 2015), indicating that abundance of sugar alcohols was affected by growing activities of organisms releasing these compounds.

Levels of arabitol were well correlated with those of mannitol ($r = 0.65$, $p < 0.01$) and erythritol ($r = 0.71$, $p < 0.01$), whereas correlation between levels of mannitol and erythritol was less significant ($r = 0.41$, $p < 0.01$). Significant correlations among these sugar alcohols were also reported for aerosols from Okinawa and Chichijima Islands, as well as global oceans (Chen et al., 2013; Fu et al., 2011; Verma et al., 2018; Zhu et al., 2015), but correlations between erythritol and mannitol (or arabitol) were occasionally less significant too (Chen et al., 2013; Verma et al., 2018). It meant that co-emissions of mannitol and arabitol always took place, while source types and/or regions sometimes might be more different for erythritol. In our study, levels of mannitol were higher for samples influenced by air masses from SCS, indicating contribution of marine sources (Fig. 5). Levels of erythritol were lower for samples influenced by air masses from SC, but comparable for samples influenced by air masses from SCS and ICP.

### 3.7. Source apportionment of POM

Five factors were resolved by PMF (Fig. 7). Factor 1 was dominated by terephthalic acid, which is commonly released by burning of plastic materials (Kawamura and Pavuluri, 2010). Contributions of vanillic acid, syringic acid, vanillin and PAHs were also significant in factor 1. Vanillic acid, syringic acid and vanillin can be derived from pyrolysis of lignin (Simoneit, 2002). PAHs are mainly produced by incomplete combustion of organic materials (Tobiszewski and Namiesnik, 2012). Thus, factor 1 should be associated with open burning of municipal waste, involving burning of plastic materials and plants. Open burning of municipal waste has been reported to be common in Southeastern Asia and rural areas of China (Kawamura and Pavuluri, 2010; Zhang et al., 2011). Factor 2 was characterized by n-alkanes, steranes and hopanes. Loadings of PAHs and LFAs were also high in factor 2. All these markers can be emitted by fossil fuel combustion (Fu et al., 2011; Kawamura et al., 2003). There could be other source types for n-alkanes, PAHs and LFAs, but steranes and hopanes are specific tracers of fossil sources (Oros and Simoneit, 2000; Rogge et al., 1993). Thus, factor 2 should be associated with fossil fuel combustion.

Factors 3 was characterized by mannitol, arabitol and erythritol, which are tracers of emissions from fungi, bacteria, marine plankton and lower plants (Bauer et al., 2008; Burshtein et al., 2011; Gosselin et al., 2016). Oleic acid also significantly contributed to factor 3, and it is derived from emissions of terrestrial plants and marine plankton (Fu et al., 2013). Factor 3 should be associated with microorganism and lower plant emissions. Factor 4 was dominated by HFAs, which represents higher plant emissions (Medeiros et al., 2006; Simoneit, 1977). LFAs was the second highest component of factor 3, followed by n-alkanes. LFAs and n-alkanes can be released by various biogenic sources and higher plants, respectively (Fine et al., 2001; Kawamura et al., 2003; Rogge et al., 1993; Rogge et al., 1991; Zhao et al., 2007a, b). So factor 4 should be associated with higher plant emissions. Factor 5 was clearly associated with biomass burning, with high loadings of typical biomass burning tracers (galactosan, mannosan and levoglucosan) (Simoneit et al., 1999), tracers of lignin pyrolysis (i.e. vanillic acid, syringic acid and vanillin) (Simoneit, 2002), and tracers of incomplete combustion of organic materials (i.e. PAHs) (Tobiszewski and Namiesnik, 2012).

So five types of POM source have been identified, and their contributions have been apportioned to be 13.21% for open burning of municipal waste (factor 1), 17.56% for fossil fuel combustion (factor 2), 27.04% for microorganism and lower plant emissions (factor 3), 30.71% for higher plant emissions (factor 4), and 11.47% for biomass
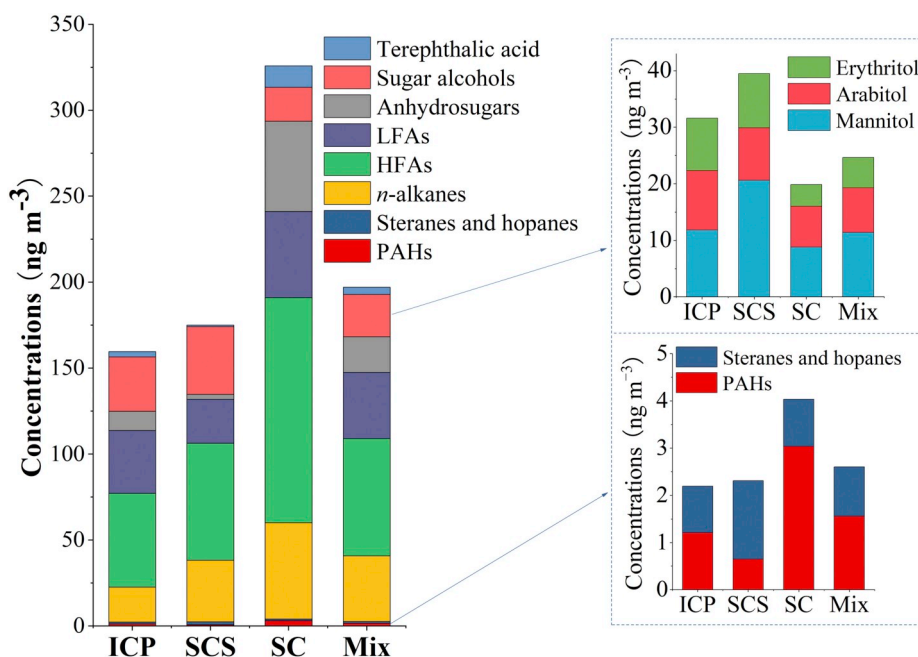
**Fig. 5.** Average molecular levels of aerosol samples influenced by air masses originaed from ICP, SCS, SC and multiple source regions (Mix).

burning (factor 5). It meant that contributions of natural (or biogenic) sources (factor 3 and 4) to POM were comparable with those of anthropogenic sources (factor 1, 2 and 5). Natural (or biogenic) sources have been reported to be significant for aerosols of islands and marine aerosols in previous studies too (Zhang et al., 2014). There was a year-round monitoring study on carbonaceous aerosols carried out recently at a background site of Hainan Island in SCS. Biogenic sources contributed to carbonaceous aerosols comparably to fossil sources or biomass burning based on radiocarbon analysis (Zhang et al., 2014). In a study of global marine aerosols, marine natural emissions contributed 4–14% to organic aerosols in coastal regions, and higher (22–33%) in North Pacific and North Atlantic (Fu et al., 2011).

It deserves our attention that continental outflow of biomass burning aerosols might be underestimated in our study. As mentioned in Section 3.1, lower levels of anhydrosugars found in April and May were likely due to a transport mechanism proposed in previous studies involving uplift and high-altitude transport of biomass burning aerosols from ICP to East Asia (Lin et al., 2009, 2013). These aerosols transported at high altitudes were overlooked for the near-ground sampling

at Xieyang Island in our study. Sampling at high elevations or sampling of wet deposition would be helpful for a better understanding of outflow of biomass burning aerosols from ICP.

In our study, microorganism and lower plant emissions concentrated in spring and summer, while other sources mostly took place in fall and winter (Fig. 8). Seasonality of microorganism and lower plant emissions seems consistent with growing activities of related organisms in different seasons. PSCF results showed that SCS and ICP were the main source regions of microorganism and lower plant emissions (Fig. 9). SC was the main source region of aerosols produced by open burning of municipal waste, biomass burning and higher plant emissions. Northern ICP also contributed a significant part of aerosols released by biomass burning and open burning of municipal waste. Source regions of fossil fuel combustion distributed not only in SC and northern ICP, but also in SCS. Marine sources of fossil fuel burning aerosols were attributed to shipping emissions. As discussed in Section 3.2, steranes and hopanes (fossil source tracers) were found to be obviously higher for samples mainly influenced by air masses from SCS, suggesting shipping emissions.

**Table 2**
PAHs diagnostic ratios of emission sources and ambient aerosol of our sampling site and other sampling sites in South China.

|  | BaA/(BaA + Chr) | IcdP/(IcdP + BghiPe) | BaP/BghiPe | Flua/(Flua + Pyr) |
|---|---|---|---|---|
| Coal combustion | 0.2–0.35[a] | – | – | – |
| Vehicular emissions | > 0.35[a] | – | – | – |
| Petrogenic | < 0.2[b] | < 0.2[b] | – | < 0.4[d] |
| Combustion | > 0.35[b] | – | – | – |
| Petroleum combustion | – | 0.2–0.5[b] | – | – |
| Grass, wood and coal combustion | – | > 0.5[b] | – | > 0.5[d] |
| Non-traffic emissions | – | – | < 0.6[c] | – |
| Traffic emissions | – | – | > 0.6[c] | – |
| Fossil fuel combustion | – | – | – | 0.4–0.5[d] |
| Xieyang Island (our study) | 0.34 ± 0.07 | 0.51 ± 0.01 | 0.34 ± 0.17 | 0.52 ± 0.02 |

Note: Diagnostic ratios used for emission sources were compiled in (Tobiszewski and Namiesnik, 2012).
–: no data.
[a] (Akyüz and Hasan, 2010).
[b] (Yunker et al., 2002).
[c] (Katsoyiannis et al., 2007).
[d] (De La Torre-Roche et al., 2009).

**Table 3**
Pearson correlations (*r* values) between levels of molecular markers.

| | Steranesand hopanes | *n*-alkanes | PAHs | LFAs | HFAs | Terephthalic acid | galactosan | mannosan | levoglucosan | mannitol | arabitol |
|---|---|---|---|---|---|---|---|---|---|---|---|
| *n*-alkanes | **0.44** | | | | | | | | | | |
| PAHs | 0.11 | **0.62** | | | | | | | | | |
| LFAs | −0.05 | 0.27 | 0.22 | | | | | | | | |
| HFAs | 0.15 | **0.74** | **0.71** | **0.36** | | | | | | | |
| terephthalic acid | 0.14 | **0.67** | **0.77** | **0.39** | **0.87** | | | | | | |
| galactosan | 0.14 | **0.67** | **0.83** | 0.30 | **0.84** | **0.87** | | | | | |
| mannosan | 0.16 | **0.64** | **0.83** | **0.32** | **0.82** | **0.85** | **0.98** | | | | |
| levoglucosan | 0.06 | **0.60** | **0.80** | **0.37** | **0.81** | **0.85** | **0.96** | **0.94** | | | |
| mannitol | **0.50** | 0.16 | −0.18 | −0.18 | −0.05 | −0.15 | −0.10 | −0.09 | −0.24 | | |
| arabitol | 0.09 | −0.10 | −0.20 | −0.20 | −0.14 | −0.17 | −0.15 | −0.16 | −0.29 | **0.65** | |
| erythritol | 0.02 | −0.29 | −0.26 | −0.27 | −0.24 | −0.22 | −0.24 | −0.24 | −0.33 | **0.41** | **0.71** |

Note: bold numbers underlined show *r* values with $p < 0.01$. HFAs: high molecular weight fatty acids; LFAs: low molecular weight fatty acids;
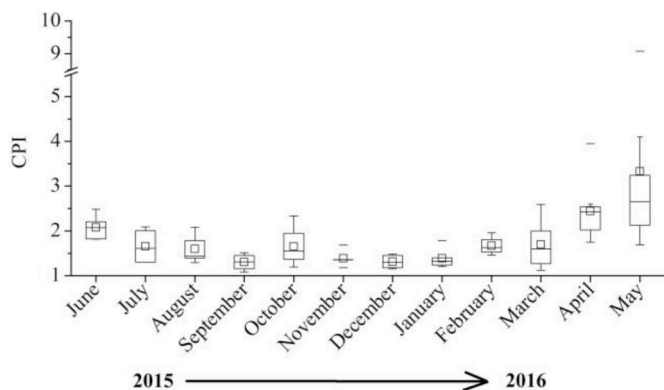


**Fig. 6.** Temporal variations of CPI values of *n*-alkanes.

## 4. Conclusion

One-year sampling of atmospheric fine particle (PM$_{2.5}$) was carried out at Xieyang Island in the northern South China Sea (SCS), an outflow region of aerosols from Indo-China Peninsular (ICP) and South China (SC). We investigated levels, sources and temporal variations of molecular markers like anhydrosugars, steranes, hopanes, PAHs, *n*-alkanes, *n*-fatty acids, sugar alcohols and so on. PMF and PSCF analysis were used to identified source types and regions of aerosol primary organic matter (POM), respectively. There were five source types contributed to aerosol POM, including open burning of municipal waste (13.21%), fossil fuel combustion (17.56%), higher plant emissions (30.71%), microorganism and lower plant emissions (27.04%) and biomass burning (11.47%). It meant contributions of anthropogenic and natural (or biogenic) sources were similar.
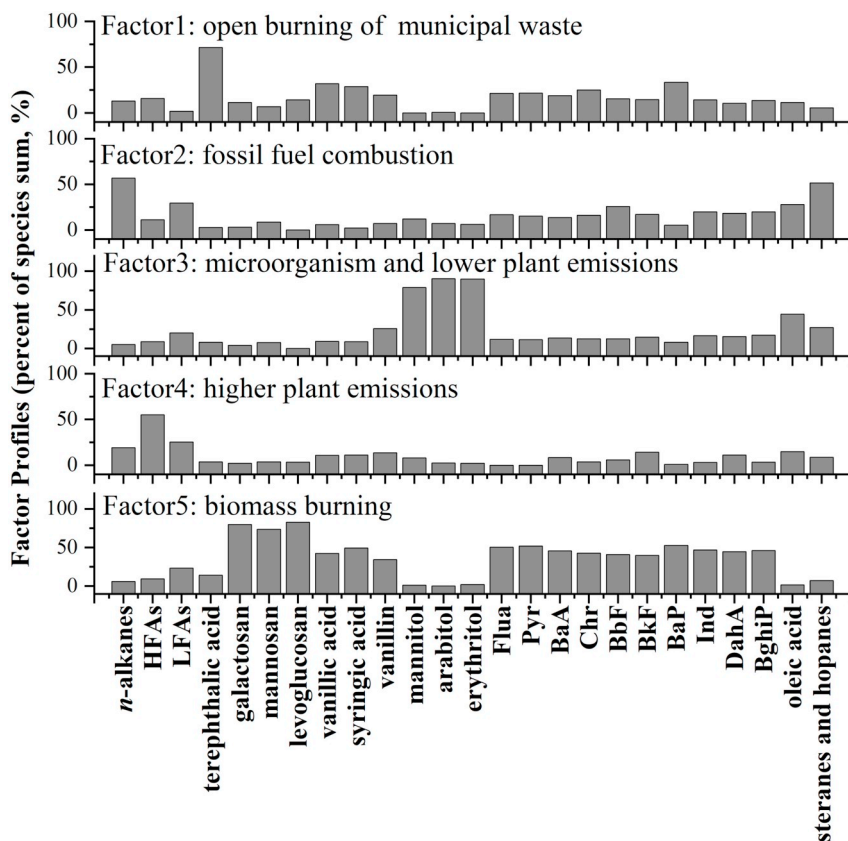


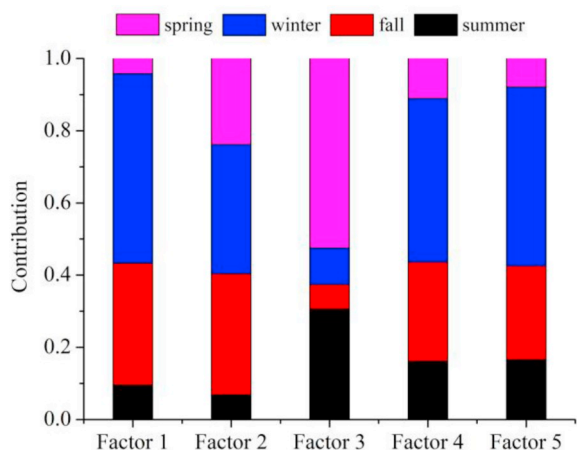**Fig. 7.** The contribution profiles of five source types identified by PMF model.

**Fig. 8.** Seasonality of contributions of five source types resolved by PMF model (Factor 1: open burning of municipal waste, Factor 2: fossil fuel combustion, Factor 3: microorganism and lower plant emissions, Factor 4: higher plant emissions and Factor 5: biomass burning).

Contributions of microorganism and lower plant emissions mainly took place in spring and summer with SCS and ICP to be the main source regions, while contributions of other source types concentrated in fall and winter with SC to be an important source region. Open burning of municipal waste, fossil fuel combustion and biomass burning were partly contributed by northern ICP too. Besides continental outflow, there were significant marine sources of fossil fuel combustion (likely shipping emissions) as well as microorganism and lower plant emissions. It was revealed by the PSCF analysis results and also higher levels of steranes and hopanes (fossil sources tracers) and mannitol (a tracer of microorganism and lower plant emissions) for aerosol samples basically influenced by air masses originated from SCS.

It deserves our attention that continental outflow of biomass burning aerosols might be underestimated in our study. Lower levels of anhydrosugars were found in April and May, when biomass burning events in ICP were most intensive and half of air masses back trajectories of our sampling site passed through ICP. This result was likely due to a transport mechanism proposed in previous studies involving uplift and high-altitude transport of biomass burning aerosols from ICP to East Asia (Lin et al., 2009, 2013). These aerosols transported at high altitudes were overlooked for the near-ground sampling at Xieyang Island. Sampling at high elevations or sampling of wet deposition would be helpful for a better understanding of outflow of biomass burning aerosols from ICP.

### Declaration of interests

The authors declare that they have no known competing financial interests or personal relationships that could have appeared to influence the work reported in this paper.
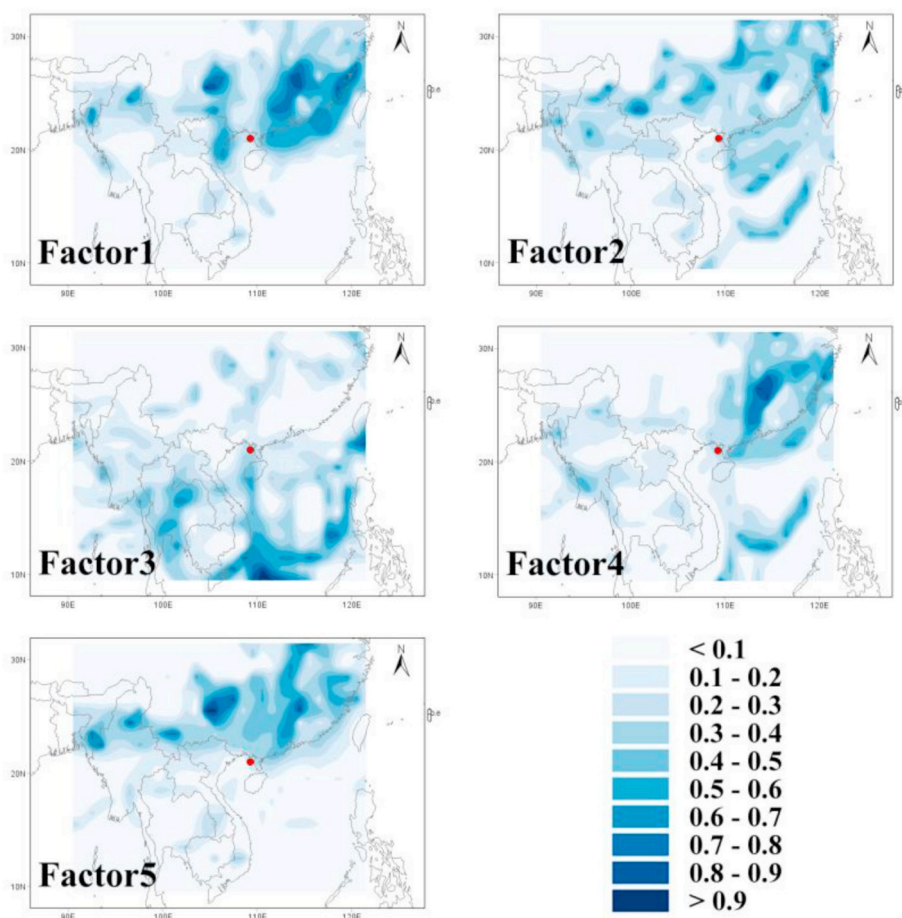


**Fig. 9.** Contributions of source regions from PSCF analysis corresponding to the five factors resolved by PMF model (Factor 1: open burning of municipal waste, Factor 2: fossil fuel combustion, Factor 3: microorganism and lower plant emissions, Factor 4: higher plant emissions and Factor 5: biomass burning).

## Acknowledgements

## Appendix A. Supplementary data

Supplementary data of this article can be found online at https://doi.org/10.1016/j.atmosenv.2019.02.033.

## References

Akyüz, M., Hasan, Ç., 2010. Gas-particle partitioning and seasonal variation of polycyclic aromatic hydrocarbons in the atmosphere of Zonguldak, Turkey. Sci. Total Environ. 408, 5550–5558.

Atwood, S.A., Reid, J.S., Kreidenweis, S.M., Cliff, S.S., Zhao, Y.J., Lin, N.H., Tsay, S.C., Chu, Y.C., Westphal, D.L., 2013. Size resolved measurements of springtime aerosol particles over the northern South China Sea. Atmos. Environ. 78, 134–143.

Bari, M.A., Baumbach, G., Kuch, B., Scheffknecht, G., 2009. Wood smoke as a source of particle-phase organic compounds in residential areas. Atmos. Environ. 43, 4722–4732.

Bauer, H., Claeys, M., Vermeylen, R., Schueller, E., Weinke, G., Berger, A., Puxbaum, H., 2008. Arabitol and mannitol as tracers for the quantification of airborne fungal spores. Atmos. Environ. 42, 588–593.

Burshtein, N., Lang-Yona, N., Rudich, Y., 2011. Ergosterol, arabitol and mannitol as tracers for biogenic aerosols in the eastern Mediterranean. Atmos. Chem. Phys. 11, 829–839.

Chan, K.L., 2017. Biomass burning sources and their contributions to the local air quality in Hong Kong. Sci. Total Environ. 596, 212–221.

Chen, J., Kawamura, K., Liu, C.-Q., Fu, P., 2013. Long-term observations of saccharides in remote marine aerosols from the western North Pacific: a comparison between 1990–1993 and 2006–2009 periods. Atmos. Environ. 67, 448–458.

Choi, J.K., Ban, S.J., Kim, Y.P., Kim, Y.H., Yi, S.M., Zoh, K.D., 2015. Molecular marker characterization and source appointment of particulate matter and its organic aerosols. Chemosphere 134, 482–491.

Chuang, M.-T., Chang, S.-C., Lin, N.-H., Wang, J.-L., Sheu, G.-R., Chang, Y.-J., Lee, C.-T., 2013. Aerosol chemical properties and related pollutants measured in Dongsha Island in the northern South China Sea during 7-SEAS/Dongsha Experiment. Atmos. Environ. 78, 82–92.

De La Torre-Roche, R.J., Lee, W.Y., Campos-Díaz, S.I., 2009. Soil-borne polycyclic aromatic hydrocarbons in El Paso, Texas: analysis of a potential problem in the United States/Mexico border region. J. Hazard Mater. 163, 946–958.

Eichler, P., Muller, M., Rohmann, C., Stengel, B., Orasche, J., Zimmermann, R., Wisthaler, A., 2017. Lubricating oil as a major constituent of ship exhaust particles. Environ. Sci. Technol. 4, 54–58.

Engling, G., Carrico, C.M., Kreldenweis, S.M., Collett, J.L., Day, D.E., Malm, W.C., Lincoln, E., Hao, W.M., Iinuma, Y., Herrmann, H., 2006. Determination of levoglucosan in biomass combustion aerosol by high-performance anion-exchange chromatography with pulsed amperometric detection. Atmos. Environ. 40, S299–S311.

Engling, G., Lee, J.J., Tsai, Y.-W., Lung, S.-C.C., Chou, C.C.K., Chan, C.-Y., 2009. Size-resolved anhydrosugar composition in smoke aerosol from controlled field burning of rice straw. Aerosol Sci. Technol. 43, 662–672.

Fabbri, D., Torri, C., Simonei, B.R.T., Marynowski, L., Rushdi, A.I., Fabianska, M.J., 2009. Levoglucosan and other cellulose and lignin markers in emissions from burning of Miocene lignites. Atmos. Environ. 43, 2286–2295.

Feng, J., Guo, Z., Chan, C.K., Fang, M., 2007. Properties of organic matter in PM2.5 at Changdao Island, China - a rural site in the transport path of the Asian continental outflow. Atmos. Environ. 41, 1924–1935.

Fine, P.M., Cass, G.R., Simoneit, B.R.T., 2001. Chemical characterization of fine particle emissions from fireplace combustion of woods grown in the northeastern United States. Environ. Sci. Technol. 35, 2665–2675.

Fine, P.M., Cass, G.R., Simoneit, B.R.T., 2002. Chemical characterization of fine particle emissions from the fireplace combustion of woods grown in the southern United States. Environ. Sci. Technol. 36, 1442–1451.

Fraser, M.P., Lakshmanan, K., 2000. Using levoglucosan as a molecular marker for the long-range transport of biomass combustion aerosols. Environ. Sci. Technol. 34, 4560–4564.

Fu, P., Kawamura, K., Miura, K., 2011. Molecular characterization of marine organic aerosols collected during a round-the-world cruise. J. Geophys. Res.-Atmos. 116, D13302.

Fu, P.Q., Kawamura, K., Chen, J., Charrière, B., Sempéré, R., 2013. Organic molecular composition of marine aerosols over the Arctic Ocean in summer: contributions of primary emission and secondary aerosol formation. Biogeosciences 10, 653–667.

Gosselin, M.I., Rathnayake, C.M., Crawford, I., Pöhlker, C., Fröhlich-Nowoisky, J.,

Schmer, B., Després, V.R., Engling, G., Gallagher, M., Stone, E., Pöschl, U., Huffman, J.A., 2016. Fluorescent bioaerosol particle, molecular tracer, and fungal spore concentrations during dry and rainy periods in a semi-arid forest. Atmos. Chem. Phys. 16, 15165–15184.

Hildemann, L.M., Markowski, G.R., Cass, G.R., 1991. Chemical-composition of emissions from urban sources of fine organic aerosol. Environ. Sci. Technol. 25, 744–759.

Hovorka, J., Pokorná, P., Hopke, P.K., Křůmal, K., Mikuška, P., Píšová, M., 2015. Wood combustion, a dominant source of winter aerosol in residential district in proximity to a large automobile factory in Central Europe. Atmos. Environ. 113, 98–107.

Jaeckels, J.M., Bae, M.S., Schauer, J.J., 2007. Positive matrix factorization (PMF) analysis of molecular marker measurements to quantify the sources of organic aerosols. Environ. Sci. Technol. 41, 5763–5769.

Jain, S., Sharma, S.K., Choudhary, N., Masiwal, R., Saxena, M., Sharma, A., Mandal, T.K., Gupta, A., Gupta, N.C., Sharma, C., 2017. Chemical characteristics and source apportionment of PM2.5 using PCA/APCS, UNMIX, and PMF at an urban site of Delhi, India. Environ. Sci. Pollut. Control Ser. 24, 14637–14656.

Jiang, H.Y., Zhong, G.C., Wang, J.Q., Jiang, H.X., Tian, C.G., Li, J., Zhao, S.Z., Yu, Z.Q., Morawska, L., Zhang, G., 2018. Using polyurethane foam-based passive air sampling technique to monitor monosaccharides at a regional scale. Environ. Sci. Technol. 52, 12546–12555.

Kang, M., Yang, F., Ren, H., Zhao, W., Zhao, Y., Li, L., Yan, Y., Zhang, Y., Lai, S., Zhang, Y., Yang, Y., Wang, Z., Sun, Y., Fu, P., 2017. Influence of continental organic aerosols to the marine atmosphere over the East China Sea: insights from lipids, PAHs and phthalates. Sci. Total Environ. 607–608, 339–350.

Katsoyiannis, A., Terzi, E., Cai, Q.Y., 2007. On the use of PAH molecular diagnostic ratios in sewage sludge for the understanding of the PAH sources. Is this use appropriate? Chemosphere 69, 1337–1339.

Kawamura, K., Ishimura, Y., Yamazaki, K., 2003. Four years' observations of terrestrial lipid class compounds in marine aerosols from the western North Pacific. Glob. Biogeochem. Cycles 17 3-1-3-19.

Kawamura, K., Pavuluri, C.M., 2010. New Directions: need for better understanding of plastic waste burning as inferred from high abundance of terephthalic acid in South Asian aerosols. Atmos. Environ. 44, 5320–5321.

Kleeman, M.J., Riddle, S.G., Robert, M.A., Jakober, C.A., 2008. Lubricating oil and fuel contributions to particulate matter emissions from light-duty gasoline and heavy-duty diesel vehicles. Environ. Sci. Technol. 42, 235–242.

Lee, C.-T., Chuang, M.-T., Lin, N.-H., Wang, J.-L., Sheu, G.-R., Chang, S.-C., Wang, S.-H., Huang, H., Chen, H.-W., Liu, Y.-L., Weng, G.-H., Lai, H.-Y., Hsu, S.-P., 2011. The enhancement of PM2.5 mass and water-soluble ions of biosmoke transported from Southeast Asia over the Mountain Lulin site in Taiwan. Atmos. Environ. 45, 5784–5794.

Lai, S., Zhao, Y., Ding, A., Zhang, Y., Song, T., Zheng, J., Ho, K.F., Lee, S.-c., Zhong, L., 2016. Characterization of PM2.5 and the major chemical components during a 1-year campaign in rural Guangzhou, Southern China. Atmos. Res. 167, 208–215.

Leung, P.Y., Wan, H.T., Billah, M.B., Cao, J.J., Ho, K.F., Wong, C.K., 2014. Chemical and biological characterization of air particulate matter 2.5, collected from five cities in China. Environ. Pollut. 194, 188–195.

Li, D., Liu, J., Zhang, J., Gui, H., Du, P., Yu, T., Wang, J., Lu, Y., Liu, W., Cheng, Y., 2017. Identification of long-range transport pathways and potential sources of PM2.5 and PM10 in Beijing from 2014 to 2015. J. Environ. Sci. 56, 214–229.

Lin, C.Y., Hsu, H.m., Lee, Y.H., Kuo, C.H., Sheng, Y.F., Chu, D.A., 2009. A new transport mechanism of biomass burning from Indochina as identified by modeling studies. Atmos. Chem. Phys. 9, 7901–7911.

Lin, N.H., Tsay, S.C., Maring, H.B., Yen, M.C., Sheu, G.R., Wang, S.H., Chi, K.H., Chuang, M.T., Ou-Yang, C.F., Fu, J.S., Reid, J.S., Lee, C.T., Wang, L.C., Wang, J.L., Hsu, C.N., Sayer, A.M., Holben, B.N., Chu, Y.C., Nguyen, X.A., Sopajaree, K., Chen, S.J., Cheng, M.T., Tsuang, B.J., Tsai, C.J., Peng, C.M., Schnell, R.C., Conway, T., Chang, C.T., Lin, K.S., Tsai, Y.I., Lee, W.J., Chang, S.C., Liu, J.J., Chiang, W.L., Huang, S.J., Lin, T.H., Liu, G.R., 2013. An overview of regional experiments on biomass burning aerosols and related pollutants in Southeast Asia: from BASE-ASIA and the Dongsha Experiment to 7-SEAS. Atmos. Environ. 78, 1–19.

Liu, J.W., Xu, Y., Li, J., Liu, D., Tian, C.G., Chaemfa, C., Zhang, G., 2014. The distribution and origin of PAHs over the asian marginal seas, the Indian, and the Pacific Oceans: implications for outflows from Asia and africa. J. Geophys. Res.-Atmos. 119, 1949–1961.

Medeiros, P.M., Conte, M.H., Weber, J.C., Simoneit, B.R.T., 2006. Sugars as source indicators of biogenic organic carbon in aerosols collected above the Howland Experimental Forest, Maine. Atmos. Environ. 40, 1694–1705.

Mochida, M., Kawamura, K., Fu, P., Takemura, T., 2010. Seasonal variation of levoglucosan in aerosols over the western North Pacific and its assessment as a biomass-burning tracer. Atmos. Environ. 44, 3511–3518.

Nguyen, D.L., Kawamura, K., Ono, K., Ram, S.S., Engling, G., Lee, C.-T., Chi, K.H., Sun, S.-A., Lin, N.-H., Chang, S.-C., Chuang, M.-T., Hsiao, T.-C., Sheu, G.-R., Ou Yang, C.-F., 2016. Comprehensive PM2.5 organic molecular composition and stable carbon isotope ratios at Sonla, Vietnam: fingerprint of biomass burning components. Aero. Air Qual. Res. 16, 2618–2634.

Nolte, C.G., Schauer, J.J., Cass, G.R., Simoneit, B.R.T., 2001. Highly polar organic compounds present in wood smoke and in the ambient atmosphere. Environ. Sci. Technol. 35, 1912–1919.

O'Dowd, C.D., de Leeuw, G., 2007. Marine aerosol production: a review of the current knowledge. Philosoph. Transact. Series A, Math, Phys., Eng. Sci. 365, 1753–1774.

O'Dowd, C.D., Facchini, M.C., Cavalli, F., Ceburnis, D., Mircea, M., Decesari, S., Fuzzi, S., Yoon, Y.J., Putaud, J.P., 2004. Biogenically driven organic contribution to marine aerosol. Nature 431, 676–680.

Oros, D.R., Abas, M.R.b., Omar, N.Y.M.J., Rahman, N.A., Simoneit, B.R.T., 2006. Identification and emission factors of molecular tracers in organic aerosols from

biomass burning: Part 3. Grasses. Appl. Geochem. 21, 919–940.

Oros, D.R., Simoneit, B.R.T., 2000. Identification and emission rates of molecular tracers in coal smoke particulate matter. Fuel 79, 515–536.

Pani, S.K., Wang, S.H., Lin, N.H., Tsay, S.C., Lolli, S., Chuang, M.T., Lee, C.T., Chantara, S., Yu, J.Y., 2016. Assessment of aerosol optical property and radiative effect for the layer decoupling cases over the northern South China Sea during the 7-SEAS/ Dongsha Experiment. Journal Of Geophysical Research-Atmospheres 121, 4894–4906.

Penner, J.E., Hegg, D., Leaitch, R., 2001. Unraveling the role of aerosols in climate change. Environ. Sci. Technol. 35, 332A–340A.

Polissar, A.V., Hopke, P.K., Paatero, P., 1998. Atmospheric aerosol over Alaska - 2. Elemental composition and sources. Journal Of Geophysical Research-Atmospheres 103, 19045–19057.

Qadir, R.M., Abbaszade, G., Schnelle-Kreis, J., Chow, J.C., Zimmermann, R., 2013. Concentrations and source contributions of particulate organic matter before and after implementation of a low emission zone in Munich, Germany. Environ. Pollut. 175, 158–167.

Ramanathan, V., Crutzen, P.J., 2003. New directions: atmospheric brown "clouds. Atmos. Environ. 37, 4033–4035.

Rogge, W.F., Hildemann, L.M., Mazurek, M.A., Cass, G.R., Simoneit, B.R.T., 1993. Sources of fine organic aerosol. 2. Noncatalyst and catalyst-equipped automobiles and heavy-duty diesel trucks. Environ. Sci. Technol. 27, 636–651.

Rogge, W.F., Hildemann, L.M., Mazurek, M.A., Cass, G.R., Simonelt, B.R.T., 1991. Sources of fine organic aerosol. 1. Charbroilers and meat cooking operations. Environ. Sci. Technol. 25, 1112–1125.

Schauer, J.J., Kleeman, M.J., Cass, G.R., Simoneit, B.R.T., 1999. Measurement of emissions from air pollution sources. 2. C-1 through C-30 organic compounds from medium duty diesel trucks. Environ. Sci. Technol. 33, 1578–1587.

Schmidl, C., Marr, I.L., Raseiro, A., Kotianová, P., Berner, A., Bauer, H., Kasper-Giebl, A., Puxbaum, H., 2008. Chemical characterisation of fine particle emissions from wood stove combustion of common woods growing in mid-European Alpine regions. Atmos. Environ. 42, 126–141.

Shi, Y., Yamaguchi, Y., 2014. A high-resolution and multi-year emissions inventory for biomass burning in Southeast Asia during 2001-2010. Atmos. Environ. 98, 8–16.

Shrivastava, M.K., Subramanian, R., Rogge, W.F., Robinson, A.L., 2007. Sources of organic aerosol: positive matrix factorization of molecular marker data and comparison of results from different source apportionment models. Atmos. Environ. 41, 9353–9369.

Simoneit, B.R.T., 1977. Organic matter in eolian dusts over the Atlantic Ocean. Mar. Chem. 5, 443–464.

Simoneit, B.R.T., 1989. Organic-matter of teh troposhere .5. application of molecular marker analysis to biogenic emissions into the troposphere for source reconciliations. J. Atmos. Chem. 8, 251–275.

Simoneit, B.R.T., 2002. Biomass burning — a review of organic tracers for smoke from incomplete combustion. Appl. Geochem. 129–162.

Simoneit, B.R.T., Schauer, J.J., Nolte, C.G., Oros, D.R., Elias, V.O., Fraser, M.P., Rogge, W.F., Cass, G.R., 1999. Levoglucosan, a tracer for cellulose in biomass burning and atmospheric particles. Atmos. Environ. 33, 173–182.

Song, J., Zhao, Y., Zhang, Y., Fu, P., Zheng, L., Yuan, Q., Wang, S., Huang, X., Xu, W., Cao, Z., Gromov, S., Lai, S., 2018. Influence of biomass burning on atmospheric aerosols over the western South China Sea: insights from ions, carbonaceous fractions and stable carbon isotope ratios. Environ. Pollut. 242, 1800–1809.

Streets, D.G., Yarber, K.F., Woo, J.H., Carmichael, G.R., 2003. Biomass burning in Asia: annual and seasonal estimates and atmospheric emissions. Glob. Biogeochem. Cycles 17, 1099.

Sullivan, A.P., Holden, A.S., Patterson, L.A., McMeeking, G.R., Kreidenweis, S.M., Malm, W.C., Hao, W.M., Wold, C.E., Collett, J.L., 2008. A method for smoke marker measurements and its potential application for determining the contribution of biomass burning from wildfires and prescribed fires to ambient PM2.5organic carbon. J. Geophys. Res.-Atmos. 113.

Tobiszewski, M., Namiesnik, J., 2012. PAH diagnostic ratios for the identification of pollution emission sources. Environ. Pollut. 162, 110–119.

Turpin, B.J., Lim, H.J., 2001. Species contributions to PM2.5 mass concentrations: revisiting common assumptions for estimating organic mass. Aerosol Sci. Technol. 35, 602–610.

Verma, S.K., Kawamura, K., Chen, J., Fu, P.Q., 2018. Thirteen years of observations on primary sugars and sugar alcohols over remote Chichijima Island in the western North Pacific. Atmos. Chem. Phys. 18, 81–101.

Wang, G., Kawamura, K., Lee, S., Ho, K., Cao, J., 2006. Molecular, seasonal, and spatial distributions of organic aerosols from fourteen Chinese cities. Environ. Sci. Technol. 40, 4619–4625.

Xiao, H.W., Xiao, H.Y., Luo, L., Shen, C.Y., Long, A.M., Chen, L., Long, Z.H., Li, D.N., 2017. Atmospheric aerosol compositions over the South China Sea: temporal variability and source apportionment. Atmos. Chem. Phys. 17, 3199–3214.

Yen, M.C., Peng, C.M., Chen, T.C., Chen, C.S., Lin, N.H., Tzeng, R.Y., Lee, Y.A., Lin, C.C., 2013. Climate and weather characteristics in association with the active fires in northern Southeast Asia and spring air pollution in Taiwan during 2010 7-SEAS/ Dongsha Experiment. Atmos. Environ. 78, 35–50.

Yunker, M.B., Macdonald, R.W., Vingarzan, R., Mitchell, R.H., Goyette, D., Sylvestre, S., 2002. PAHs in the Fraser River basin: a critical appraisal of PAH ratios as indicators of PAH source and composition. Org. Geochem. 33, 489–515.

Zhang, F., Chen, Y.J., Chen, Q., Feng, Y.L., Shang, Y., Yang, X., Gao, H.W., Tian, C.G., Li, J., Zhang, G., Matthias, V., Xie, Z.Y., 2018. Real-world emission factors of gaseous and particulate pollutants from marine fishing boats and their total emissions in China. Environ. Sci. Technol. 52, 4910–4919.

Zhang, G., Li, J., Li, X.D., Xu, Y., Guo, L.L., Tang, J.H., Lee, C.S.L., Liu, X.A., Chen, Y.J., 2010. Impact of anthropogenic emissions and open biomass burning on regional carbonaceous aerosols in South China. Environ. Pollut. 158, 3392–3400.

Zhang, T.T., Fiedler, H., Yu, G., Ochoa, G.S., Carroll, W.F., Gullett, B.K., Marklund, S., Touati, A., 2011. Emissions of unintentional persistent organic pollutants from open burning of municipal solid waste from developing countries. Chemosphere 84, 994–1001.

Zhang, Y., Yang, X., Brown, R., Yang, L.P., Morawska, L., Ristovski, Z., Fu, Q.Y., Huang, C., 2017. Shipping emissions and their impacts on air quality in China. Sci. Total Environ. 581, 186–198.

Zhang, Y.L., Li, J., Zhang, G., Zotter, P., Huang, R.J., Tang, J.H., Wacker, L., Prevot, A.S.H., Szidat, S., 2014. Radiocarbon-based source apportionment of carbonaceous aerosols at a regional background site on hainan island, south China. Environ. Sci. Technol. 48, 2651–2659.

Zhang, Y.N., Zhang, Z.S., Chan, C.Y., Engling, G., Sang, X.F., Shi, S., Wang, X.M., 2012. Levoglucosan and carbonaceous species in the background aerosol of coastal southeast China: case study on transport of biomass burning smoke from the Philippines. Environ. Sci. Pollut. Control Ser. 19, 244–255.

Zhao, X., Wang, X., Ding, X., He, Q., Zhang, Z., Liu, T., Fu, X., Gao, B., Wang, Y., Zhang, Y., Deng, X., Wu, D., 2014. Compositions and sources of organic acids in fine particles (PM2.5) over the Pearl River Delta region, south China. J. Environ. Sci. 26, 110–121.

Zhao, Y., Hu, M., Slanina, S., Zhang, Y., 2007a. Chemical compositions of fine particulate organic matter emitted from Chinese cooking. Environ. Sci. Technol. 41, 99–105.

Zhao, Y., Hu, M., Slanina, S., Zhang, Y., 2007b. The molecular distribution of fine particulate organic matter emitted from Western-style fast food cooking. Atmos. Environ. 41, 8163–8171.

Zhao, Y., Zhang, Y., Fu, P., Ho, S.S.H., Ho, K.F., Liu, F., Zou, S., Wang, S., Lai, S., 2016. Non-polar organic compounds in marine aerosols over the northern South China Sea: influence of continental outflow. Chemosphere 153, 332–339.

Zheng, L., Yang, X., Lai, S., Ren, H., Yue, S., Zhang, Y., Huang, X., Gao, Y., Sun, Y., Wang, Z., Fu, P., 2018. Impacts of springtime biomass burning in the northern Southeast Asia on marine organic aerosols over the Gulf of Tonkin, China. Environ. Pollut. 237, 285–297.

Zhu, C.M., Kawamura, K., Kunwar, B., 2015. Organic tracers of primary biological aerosol particles at subtropical Okinawa Island in the western North Pacific Rim. J. Geophys. Res.-Atmos. 120, 5504–5523.

Zong, Z., Wang, X., Tian, C., Chen, Y., Qu, L., Ji, L., Zhi, G., Li, J., Zhang, G., 2016. Source apportionment of PM2.5 at a regional background site in North China using PMF linked with radiocarbon analysis: insight into the contribution of biomass burning. Atmos. Chem. Phys. 16, 11249–11265.